Graftable chiral ligands for surface organometallic materials: calixarenes bearing asymmetric centers directly attached to the lower rim†

Andrew Solovyov, Justin M. Notestein,‡ Kathleen A. Durkin§ and Alexander Katz*

Received (in Montpellier, France) 25th January 2008, Accepted 14th March 2008
First published as an Advance Article on the web 29th May 2008
DOI: 10.1039/b801434p

A family of chiral lower-rim substituted calixarene ligands **1–14** is synthesized and characterized as prospective ligands for synthesis of asymmetric active sites for heterogeneous catalysis and adsorption using a surface organometallic approach. The ligands possess asymmetric centers directly attached to lower-rim oxygens; the asymmetric centers are tailored with sterically bulky naphthyl and electron withdrawing CF_3 substituents. ^1H and ^{13}C NMR spectroscopies demonstrate that mono- and 1,3-di-alkylated calixarenes synthesized using this procedure adopt the cone-shaped conformation, which is stabilized by multiple hydrogen bonds at the lower rim. Smaller pendant groups and polar solvents increase the dialkylation/monoalkylation ratio. The reaction proceeds with full inversion of configuration as established *via* single crystal X-ray diffraction of an *N*-Cbz-protected aminocyclopentoxy-modified calixarene. The calixarenes synthesized by this approach are characterized using circular dichroism (CD) spectroscopy and *ab initio* modeling, which is used to identify the minimal molecular fragment responsible for the observed lowest energy Cotton effect in the CD spectrum. Factors that influence the intramolecular induction of asymmetry throughout the calixarene scaffold are investigated by systematically varying substituent steric bulk, connectivity of the asymmetric center to the calixarene core, and the extent of hydrogen bonding at the calixarene lower rim. The asymmetry of the calixarene core is quantified using ^1H NMR spectroscopic shifts of aromatic *meta* and methylene bridge hydrogens and supported using *ab initio* calculations. The results demonstrate that calixarene core asymmetry is most strongly induced for rigid calixarene cores—an attribute that is expected to be preserved upon metal complexation and anchoring of these prospective ligands.

Introduction

The high proficiency and enantioselectivity of biological catalysts is thought to be the result of precise organization of chemical functionality in the inner and outer spheres surrounding active sites. An open question is the minimum degree of structural complexity necessary for achieving enhanced catalytic function due to this cooperativity.[1] Inspired by metal atom isolation within the chiral environment of metalloenzymes such as vanadium bromoperoxidase,[2] this manuscript reports the design and synthesis of a family of functionalized calixarenes that are envisaged for metal binding within a molecular scaffold having arranged chiral groups, which are directly connected to ether oxygens, all while grafted on heterogeneous surfaces (Fig. 1). For such materials containing early transition metals,[3] it has been recently shown that the metal and ether oxygens are in dative contact, which should facilitate induction of chiral information from pendant groups to the calixarene core and the bound metal. This approximate geometry has been explored somewhat in enantioselective catalysis, including homogeneous inorganic[4] and surface-organometallic catalysts,[5] and a Ti(IV)–calixarene catalyst with chiral groups at the lower rim,[6] as well as in epoxidation reaction intermediates such as chiral organic peroxide-bound Ti(IV) centers, which demonstrate enhanced reaction enantioselectivity upon anchoring in confined pores.[7,8] Here, we demonstrate the stereoselective synthesis of a new family of C_2-symmetric calixarene ligands, which is known to be a desired symmetry for chiral catalysts.[9] Calixarenes have been synthesized previously with lower rim, tetrahedral chiral centers and with topologically chiral arrangements, but in many of these examples,[10–12] the chiral center is not directly attached to a calixarene phenol oxygen, limiting potential dative contacts with metals bound at adjacent phenolates. Our synthetic approach builds on the results of Ungaro and colleagues who have synthesized calix-sugars consisting of an asymmetric center directly attached to the calixarene lower rim,[13,14] and uses the Mitsunobu reaction for ligand synthesis. We quantify the transfer of asymmetry throughout the entire calixarene scaffold using the chemical shifts of diastereotopic hydrogens

Department of Chemical Engineering, University of California, Berkeley, CA 94720-1462, USA. E-mail: katz@cchem.berkeley.edu
† Electronic supplementary information (ESI) available: General experimental methods and X-ray crystallographic information for **2** and **7**; ^1H NMR, ^{13}C NMR, 2D ^1H COSY NMR spectra of new compounds **1–14**; Chiral HPLC for racemic- and (*S*,*S*)-**2**; experimental CD and UV-Vis spectra for compounds **6** and **14**. CCDC reference numbers 685846 and 685847. See DOI: 10.1039/b801434p
‡ Current address: Department of Chemical and Biological Engineering, Northwestern University, 2145 Sheridan Road, Evanston, IL 60208-3120, USA.
§ Current address: College of Chemistry, University of California, Berkeley, CA 94720-1462, USA.

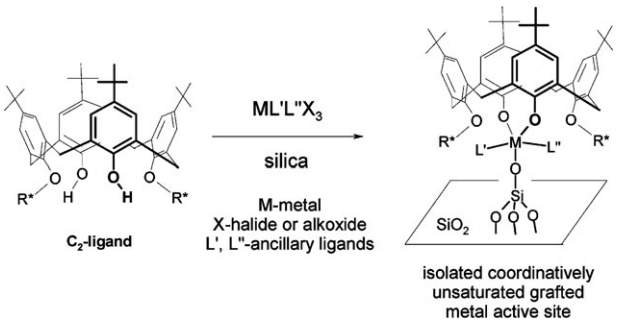

Fig. 1 Envisaged surface organometallic materials based on the C_2-symmetric ligands described in this manuscript.

on the calixarene core, circular dichroism spectroscopy, and density functional theory (DFT). This is performed to elucidate the critical structural characteristics, such as rigidity and atomic connectivity, that control the transfer of asymmetry within the cone conformer of the calixarene.

Results and discussion

Molecule synthesis and characterization

Williamson-type nucleophilic substitution reactions have been used for introducing tethered chiral centers to the lower rim of calixarenes *via* methylene and carbonyl spacers,[15–17] but examples in which chiral centers are directly attached to lower rim oxygens are relatively rare.[13,14,18] A particularly pertinent example on the synthesis of such a calixarene relies on inversion of configuration under Williamson type reaction conditions when treating *p-tert*-butylcalixarene with ethyl (*S*)-*O*-tosyllactate. Communication of asymmetry throughout the whole molecule was shown in this example *via* the diastereotopism of calixarene scaffold hydrogens.[18] We initially attempted to generalize this reaction procedure by implementing chiral naphthyl bromides as alkylating agents; however, these attempts were unsuccessful due to racemization of the chiral halide under alkylation reaction conditions. Indeed, under reaction conditions required by the Williamson-type nucleophilic substitution, the general stereochemical stability of compounds in which the stereogenic center is directly attached to a good leaving group (halogen, triflate, tosylate) was equally poor.

The Mitsunobu protocol has been previously used to functionalize calixarene lower rims with alkyl groups[19–23] and stereoselectively with glycosides;[13,14] in this manuscript, we use the Mitsunobu reaction to synthesize calixarenes **1–14**, which possess bulky aromatic substituents at each chiral carbon on the lower rim, by employing commercially available secondary alcohols, which are not prone to racemization. The reaction of *p-tert*-butylcalixarene with chiral alcohols in the presence of 3 equivalents of diethyl azodicarboxylate (DEAD)–PPh_3 proceeded regioselectively in THF at room temperature (Scheme 1). The products of this reaction were distally disubstituted lower rim calixarenes **1–4** and **8**, which were synthesized in yields of greater than 60%, and a small amount (typically less than 5%) of monosubstituted calixarene (Table 1). Dialkylation of *tert*-butylcalixarene with three

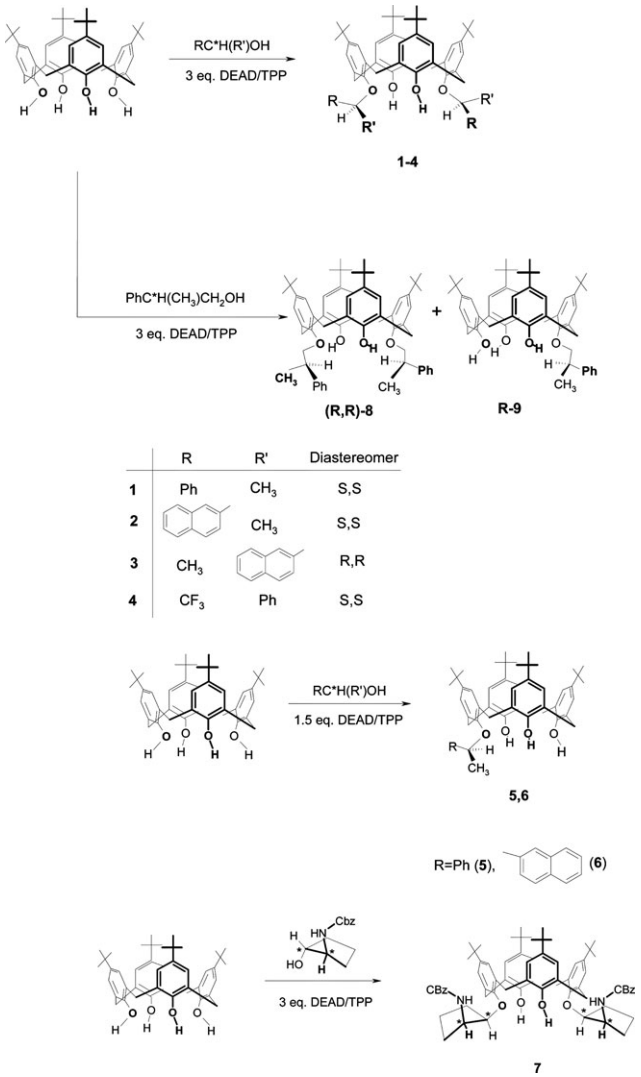

	R	R'	Diastereomer
1	Ph	CH_3	S,S
2		CH_3	S,S
3	CH_3		R,R
4	CF_3	Ph	S,S

Scheme 1

equivalents of alcohol proceeded relatively slowly *via* sequential alkylation. After 8 h, dialkylated **8** represented 31% of the reaction mixture containing mono- and dialkylated calixarenes. After 24 h, the reaction was almost complete with **8** representing 95% of the mixture consisting of dialkylated **8** and monoalkylated **9**. Monosubstituted calixarenes **5** and **6** were synthesized as sole products in 47% and 44% yield, respectively, by decreasing the amount of DEAD–TPP to 1.5 equivalents per calixarene. A prolonged reaction time in this case did not affect yields. The final reaction mixture contained product, unreacted *tert*-butylcalixarene and only trace amounts of disubstituted product. FAB MS of the crude reaction mixture showed no evidence for the formation of higher alkylated analogs, likely because of the lower reactivity of subsequent OH groups on the calixarene lower rim[24] due to steric crowding and lower acidity. Electron withdrawing CF_3 substituents in compound **4** were attached with yields similar to compound **1**.

Though a high degree of stereoselectivity is preserved during the reaction, changing the upper rim substitution pattern from *tert*-butyl groups to H greatly decreases the degree of

Table 1 Reaction conditions and yields of **1–13**. Compounds **1–6** and **8–13** were synthesized at room temperature, and compound **7** was synthesized at 80 °C.

Compound	*para*-Substitution	DEAD/TPP (eq)	Solvent	Time/h	Yield (%)
1	*tert*-C_4H_9	3	THF	24	60
2	*tert*-C_4H_9	3	THF	24	75
3	*tert*-C_4H_9	3	THF	24	70
4	*tert*-C_4H_9	3	THF	24	60
5	*tert*-C_4H_9	1.5	THF	24	47
6	*tert*-C_4H_9	1.5	THF	24	44
7	*tert*-C_4H_9	1.5	Toluene	2	8
8	*tert*-C_4H_9	3	THF	24	80
9	*tert*-C_4H_9	1.5	THF	8	42
10	H	3	Benzene	2	55
11	H	3	THF	24	30
12	H	3	THF	24	42
13	H	1.5	THF	24	47

alkylation. Indeed, using *R*-1-phenylethanol, isolated yields of di- and mono-substituted calixarenes **12** and **13** are 42% and 47%, respectively, using the same reaction conditions as described above for di- and mono-alkylation. However, the more sterically bulky *R*-1-(α-naphthyl)ethanol leads to formation of an equimolar mixture of mono- and di-substituted cone calixarenes **10** and **11** (30% yield for each), even when using the same reaction conditions as used above for dialkylation, involving a three-fold excess of DEAD–TPP. Decreasing the solvent polarity from THF to benzene allows isolation of mono-substituted calixarene **10** as the sole product in 55% yield under otherwise identical conditions (Scheme 2).

All resulting mono- and 1,3-di-alkylated products exist in the cone conformation in which calixarene aromatic rings are in a *syn* orientation, as evidenced *via* ^{13}C NMR spectra that contain distinctive methylene carbon resonances near 31 ppm,[25] and a characteristic pattern of resonances in the ^1H NMR spectra. Specifically, the resonances for axial and equatorial methylene hydrogens are shifted relative to each other, which reflects the influence of the lower rim substitution pattern and the dihedral angle between neighboring aromatic rings on the calixarene.[26] The chemical shift differences range from 0.68 ppm–1.24 ppm, which are consistent with the cone conformation. The X-ray crystallographic structure of molecule **2** crystallized from acetonitrile is shown in Fig. 2 and demonstrates the cone conformer of **2** to be rigidified *via* two intramolecular hydrogen bonds on the lower rim.[27]

The Mitsunobu reaction described above for **2** is highly stereoselective, with a measured diastereomeric excess (de) *via* chiral HPLC of greater than 98%, which appears to be limited only by the optical purity of alcohol reactant. Although the Mitsunobu reaction typically proceeds *via* S_N2 mechanism with full inversion of configuration at the asymmetric center,[28] retention of configuration in the Mitsunobu reaction has been observed when using reactants with sterically bulky substituents.[29] Absolute stereochemistry was established here using single-crystal X-ray diffraction of the sterically bulky *N*-benzyloxycarbonylaminocyclopentoxy-modified calixarene **7**. The structure derived from single crystal X-ray diffraction of crystals grown from ethanol is shown in Fig. 3 and consists exclusively of the *cis* form of the *N*-Cbz-protected aminocyclopentanol units attached to the calixarene lower rim.[30] This

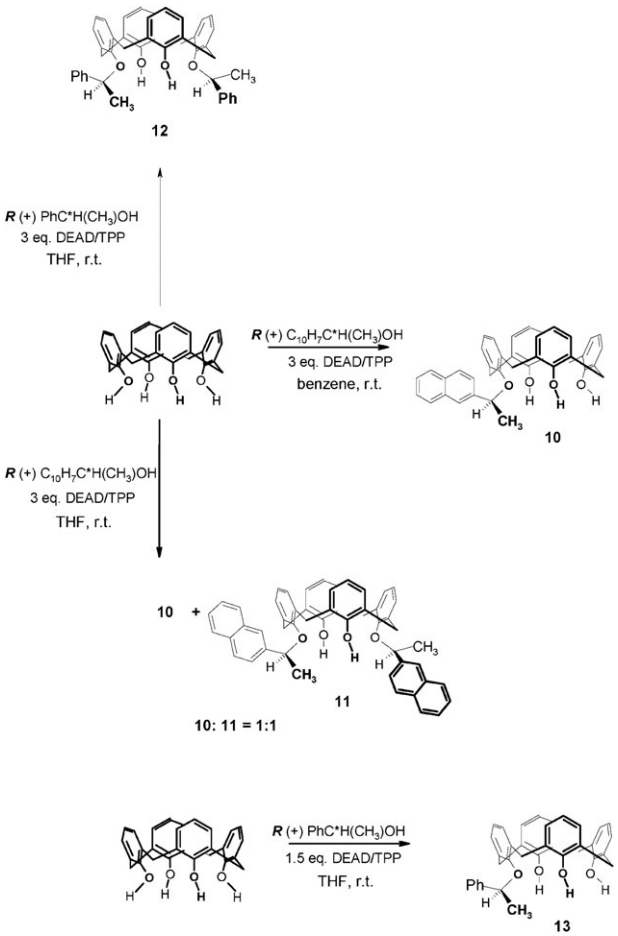

Scheme 2

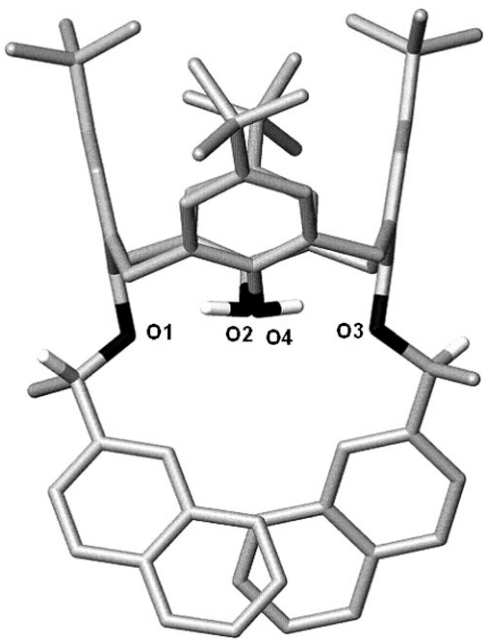

Fig. 2 Structure of **2** as determined *via* single-crystal X-ray diffraction. Hydrogens have been omitted for clarity except those connected to chiral carbons and phenolic oxygens. An acetonitrile molecule inside of the calixarene cavity has been omitted for clarity.†

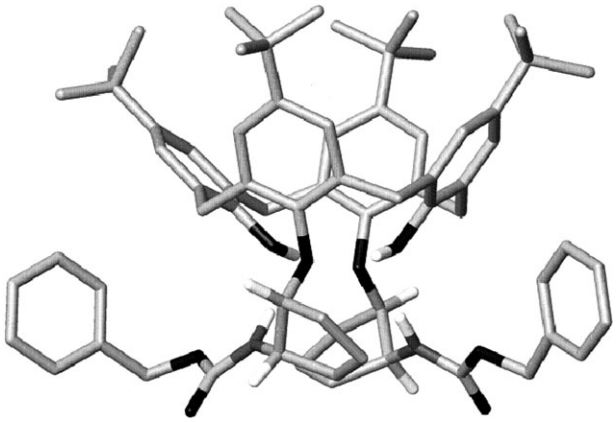

Fig. 3 Structure of **7** as determined *via* single-crystal X-ray diffraction. Hydrogens have been omitted for clarity except those connected to chiral carbons, amide nitrogens, and phenolic oxygens. Disordered ethanol molecules have been omitted for clarity.†

proves that full inversion of configuration occurs at the chiral carbon connected to the calixarene lower rim oxygen.

Diastereotopic hydrogens

Diastereotopism of hydrogens in disubstituted compounds **1–4**, **8**, **11**, **12**, **14**, **15** is used to quantify the degree of induction of asymmetry throughout the entire calixarene molecule. Diastereotopic hydrogens are manifested in two regions of the ^{1}H NMR spectrum representing: (i) methylene bridge hydrogens appearing as four doublets (two AB spin systems) corresponding to two sets of diastereotopically inequivalent axial and equatorial hydrogens; (ii) aromatic *meta*-hydrogens appearing as four doublets corresponding to two sets of diastereotopically inequivalent hydrogens on substituted and unsubstituted phenols. Chemical shift differences for diastereotopic hydrogens in all disubstituted cone calixarene products are represented in Table 2. It is informative to compare the diastereotopism of hydrogens in compounds **1** and **8** because they differ only in the presence of a single methylene spacer between the asymmetric center and calixarene lower rim oxygen and thus provide insight into the role of flexibility surrounding the asymmetric center. The corresponding ^{1}H NMR spectra are shown in Fig. 4 and demonstrate that the methylene bridge hydrogens in **8** are split by a $\Delta\delta_{ax}$ of 0.20 ppm for axial hydrogens and $\Delta\delta_{eq}$ of 0.05 ppm for equatorial hydrogens, whereas the corresponding values for **1** are $\Delta\delta_{ax}$ of 0.71 ppm and $\Delta\delta_{eq}$ of 0.35 ppm. The much larger chemical shift differences for the more rigid **1** are also manifested in the aromatic *meta*-hydrogens, for which the chemical shift differences in **8** are 0.02 ppm (substituted aromatic rings) and 0.05 ppm (unsubstituted aromatic rings), compared with 0.12 ppm (substituted) and 0.15 ppm (unsubstituted) in **1**. Altogether, these results demonstrate that the greater flexibility *via* presence of a single methylene spacer in **8** acts to significantly decrease diastereotopic chemical shift differences relative to **1**. Comparison of other calixarenes such as **1** and **2** demonstrates that larger steric bulk of substituents (naphthyl *versus* phenyl) at the asymmetric center also increases the chemical shift difference of diastereotopic hydrogens. This is consistent with previously noted general trends, for which chemical shift differences of diastereotopic hydrogens were larger in molecules that consisted of asymmetric centers having substituents of bulkier size.[31] Finally, for all *tert*-butyl-calixarene compounds, aromatic *meta*-hydrogens on the unsubstituted rings, which are located slightly further away from the chiral centers, have a larger chemical shift difference compared to their substituted counterparts, as observed previously for **15**.[18] However, in contrast to its *tert*-butylated analog, **2**, *para*-unsubstituted calixarene **11** exhibits differences in chemical shifts ($\Delta\delta$) for resonances of diastereotopic *meta*-hydrogens that are almost the same for substituted and unsubstituted aromatic units in **11**. The *meta*-hydrogens in **11** have a $\Delta\delta$ value of 0.21 ppm. This is the largest difference in chemical shift ($\Delta\delta$) for diastereotopic *meta*-hydrogens of all of the disubstituted chiral calixarenes investigated here, and appears to be the largest reported to date for a calixarene, which were measured to be 0.06 ppm and 0.08 ppm for *meta*-hydrogens on substituted and unsubstituted aromatic rings, respectively, in the ethyl lactate derivative consisting of **15**.[18]

The effect of lower-rim hydrogen bonding on chirality induction is demonstrated by comparison of **2** to the trifluoromethyl-containing **4** and the propoxylated lower rim analog **14**. Replacing the CH_3 in **2** with CF_3 in **4** decreases the extent of lower-rim intramolecular hydrogen bonding, as demonstrated by the 1.62 ppm upfield shift in the lower-rim phenoxy ^{1}H NMR resonance relative to **2**, which is attributed to polarization caused by the CF_3 group. Values of $\Delta\delta$ of 0.01 ppm (substituted) and 0.09 ppm (unsubstituted) were measured for *meta*-hydrogens in **4**, which represent at least a two-fold decrease compared with values for **2**. Capping the two remaining lower-rim OH groups in **2** *via* alkylation with 1-bromopropane in the presence of sodium hydride as represented in Scheme 3 leads to a more conformationally mobile

Table 2 Chemical shifts of methylene bridges and aromatic *meta*-hydrogens for 1,3-disubstituted calixarenes **1, 2, 4, 8, 11, 12, 14, 15** as measured by ^{1}H NMR spectroscopy

No.	Chiral fragment	*p*-	δ_{ax}	δ_{eq}	$\Delta\delta$ArH$_{unsub}$	[a]$\Delta\delta$ArH$_{sub}$
1	(*S*,*S*)-CH(CH$_3$)Ph	*t*-Bu	3.82, 4.53	2.94, 3.29	0.15	0.12
2	(*S*,*S*)-CH(CH$_3$)C$_{10}$H$_7$	*t*-Bu	3.89, 4.58	2.85, 3.35	0.19	0.18
4	(*S*,*S*)-CH(CF$_3$)C$_{10}$H$_7$	*t*-Bu	3.79, 4.50	3.11, 3.33	0.09	0.01
8	(*R*,*R*)-CH$_2$CH(CH$_3$)Ph	*t*-Bu	4.15, 4.35	3.25, 3.30	0.05	0.02
11	(*S*,*S*)-CH(CH$_3$)C$_{10}$H$_7$	H	3.85, 4.60	2.87, 3.41	0.21	0.21
12	(*S*,*S*)-CH(CH$_3$)Ph	H	3.78, 4.56	2.94, 3.38	0.16	0.16
14	(*S*,*S*)-CH(CH$_3$)C$_{10}$H$_7$	*t*-Bu	4.19, 4.59	2.73, 3.20	0.12	0.10
15[18]	(*R*,*R*)-CH(CH$_3$)CO$_2$Et	*t*-Bu	4.35, 4.45	3.32, 3.33	0.08	0.06

[a] The substituted rings are defined as those which are directly connected to the chiral center.

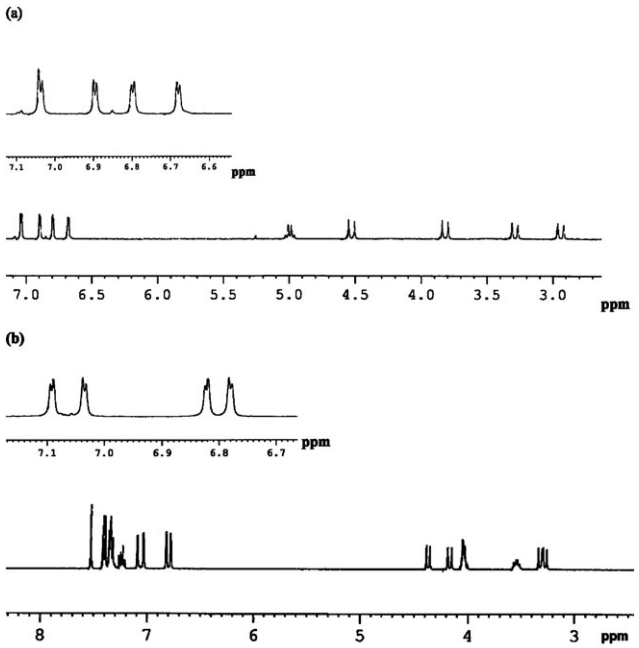

Fig. 4 Resonances in the methylene and aromatic regions of the ^{1}H NMR of **1** (a) and **8** (b) in $CDCl_3$. All relevant resonances are labeled in Table 1.

calixarene due to lack of stabilization *via* lower-rim hydrogen bonding. This lack of rigidity in tetraalkylated calixarenes has been previously demonstrated in the low temperature flattened cone–flattened cone interconversions of tetrapropoxy calixarenes.[32] While **14** remains in the cone conformer based on the presence of an AB spin system of methylene resonances in the ^{1}H NMR spectrum, there is a drop of at least 1.5-fold in $\Delta\delta$ for aromatic *meta* hydrogens relative to **2**. The observations above underline the important role of hydrogen bonding in increasing conformational rigidity for maximizing chiral induction, and are supported by recent observations on the importance of hydrogen bonding for regulating molecular conformations and enhancing axial chirality induction in biphenyldiols.[33]

Asymmetry is also transferred throughout the calixarene scaffold in monosubstituted compounds such as **10**, in which four pairs of doublets can be assigned to each $ArCH_2Ar$ methylene group by 2D COSY ^{1}H NMR spectroscopy. The cone conformation of mono-alkylated calix[4]arene **10** is supported by the presence of four pairs of doublets (2.86, 3.39, 3.47, 3.54 for the diastereotopic equatorial hydrogens and 3.67, 4.15, 4.33, 4.76 for the diastereotopic axial hydrogens), with a chemical shift difference between axial and equatorial resonances ranging from 0.75 ppm–1.22 ppm. Additionally in triol **10**, low field resonances of the three OH

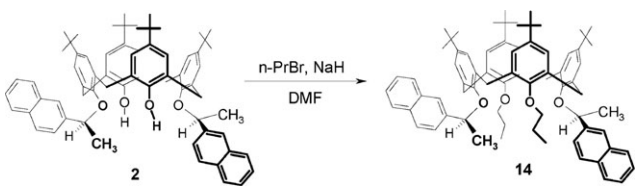

Scheme 3

hydrogens beyond 9 ppm reflect stabilization of the cone conformation *via* hydrogen bonding at the lower rim.

DFT based GIAO calculations were performed on several calixarenes in an attempt to isolate electronic effects that may explain the observed results in Table 2. Chemical shift differences are compared: (i) between axial and equatorial hydrogens attached to a single methylene bridge, which are reflective of the cone conformation of the calixarenes investigated; and (ii) between axial hydrogens and equatorial hydrogens attached to proximal methylene bridge carbons on the calixarene scaffold, which are reflective of diastereotopism. Each of these molecules exhibits a range of possible conformations in the calculated gas phase. In **2**, conformational variability is observed, and high level calculations are subsequently performed on the four lowest energy conformers. Molecule **4** is found to be the most amenable to higher level calculation having only one low energy conformer. The calculated differences in chemical shift between axial and equatorial methylene bridge hydrogens in **4** are 1.83 ppm and 0.58 ppm, respectively, as compared to the experimentally measured values of 1.17 ppm and 0.68 ppm corresponding to the cone conformer. We note that smaller chemical shift differences are observed for the axial/equatorial methylene pair that is most exposed to the ring current of the naphthyl. The distances from the axial hydrogens to a centroid defined by the six carbons comprising the proximal phenyl of the naphthyl ring are 3.4 Å *versus* 5.6 Å, and it is the shorter distance that is influenced by the ring current effect. The same effect is observed in **7**, **8**, and **2**, although the calculated effect is less pronounced in **2** (experimental: 1.23 ppm and 1.04 ppm *versus* calculated values (for lowest *E* conformer) of 1.58 ppm and 1.22 ppm).

In addition to calculating chemical shift differences between axial and equatorial hydrogens on the same methylene bridge carbon above, calculated diastereotopic chemical shift differences in methylene bridge hydrogens are compared to experimental values for the axial/axial as well as equatorial/equatorial hydrogens on proximal methylene bridge carbons. In **4**, the experimental $\Delta\delta_{ax}$ is 0.71 ppm whereas the calculated value is 1.42 ppm. For the equatorial hydrogens, the experimental $\Delta\delta_{eq}$ is 0.22 ppm whereas the calculated value is 0.34 ppm. Though the calculated results above cannot be explained as an obvious result of any one isolated electronic contribution, the unification of the calculated results clearly matches the experimentally observed trend of $\Delta\delta_{ax}$ being greater $\Delta\delta_{eq}$. Progress towards routinely calculating diastereotopic chemical shift differences for structures such as **4** and **2** is evident by the fact that not that long ago, these types of calculations were impossible.[31]

CD Spectroscopy

Fig. 5a contains CD spectra measured for **2** and **3** in dichloromethane. The magnitude of the molar ellipticities are significantly greater than those previously reported for lower rim substituted calixarenes bearing a chiral carbon β to the calixarene phenol.[16] The symmetry of these spectra, particularly within the range of 260 nm to 285 nm, is consistent with the high optical purity of the compounds as supported by chiral HPLC data discussed above. To identify the minimal

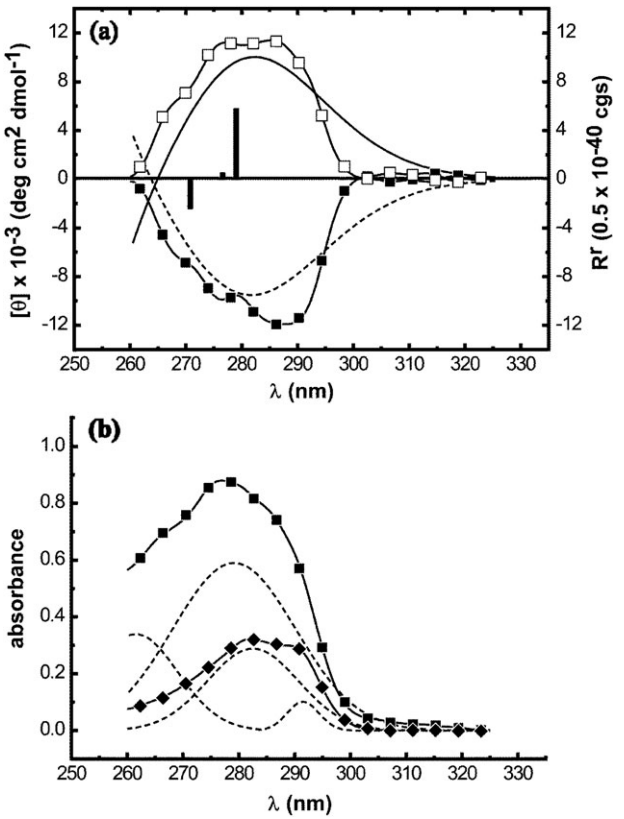

Fig. 5 (a) Experimental CD spectra of **2** (□) and **3** (■) compared to simulated CD spectra of optimized *S*-**16** (—) and its optimized *R*-enantiomer (—). Bars represent simulated rotary strengths and relative energies for optimized S-**16**. The energies of the simulated transitions for the fragments have been increased by 0.17 eV to match the simulated lowest energy transition with experimentally measured lowest energy naphthyl-centered transition at 279 nm.[34] (b) UV-visible spectra of **2** (■) and *tert*-butylcalix[4]arene (♦). The individual transitions for **2**, as determined from non-linear regression, are shown as dashed curves.

molecular fragment responsible for the origin of the optically active transitions, the UV-visible spectra of all calixarene compounds are analyzed by deconvoluting the spectra as a sum of Gaussian distributions around transitions centered at 262 nm, 279 nm, 282 nm and 293 nm, within a 1 nm tolerance. Transitions at 282 nm and 293 nm for unmodified *tert*-butylcalixarene are used to fix the corresponding transitions for modified calixarene compounds such as **2** (Table 3, Fig. 5). The transitions at 279 nm and 262 nm in the UV-visible spectra are specific to calixarene compounds bearing pendant naphthalene rings, including **6** and **14** (see ESI†). The molar ellipticities corresponding to the lowest energy transition specific to the naphthalene systems (279 nm) are listed in Table 3. It is apparent from these data that all compounds with absolute *S*-configuration produce a positive molar ellipticity at 279 nm. Notably, the molar ellipticity of the chiral alcohol precursor 1-(α-naphthyl)ethanol is eight-fold weaker than the naphthyl-containing calixarene compounds, despite a similar extinction coefficient in the deeper ultraviolet region of the UV-Vis spectrum. This suggests that the optically active transitions of the naphthyl-modified calixarenes are strongly dependant on the electronic interactions between the calixarene and naphthalene π systems.

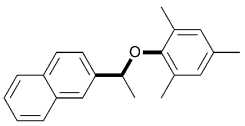

16

The *S*-enantiomer molecule of **16** captures this minimal arene–naphthalene connectivity and is therefore chosen for *ab initio* calculations for understanding the effect of the absolute conformation of the chiral carbon on the circular dichroism spectrum of the substituted calixarenes. Both enantiomers of **16** are optimized at the DFT/B3LYP/6-31 + G* level of theory to a dihedral angle of −160° and +160°, respectively, around the phenyl–O–CH(CH_3)–naphthyl bonds (as marked). A molecular mechanics conformational search on the full structure of **2** reveals two broad energy minima corresponding to dihedral angles −150° and −88°. The overall sign and magnitudes of the simulated circular dichroism spectra of the fragment above are very weakly dependent on this dihedral angle (−160°, −150°, or −88°), so results for the single, optimized structure are chosen to approximate the Boltzmann average of all possible conformations that may exist in solution for this fragment.

Within the energy range of the experimental spectra, TD-DFT simulated spectra of **16** are characterized by a prominent, large positive rotation at ∼4.2 eV followed by a series of weakly positive or negative rotations. TD-DFT methods are known to typically underestimate energies of π–π* transitions, so the energies of simulated transitions were increased by ∼0.2 eV,[34] making the simulated lowest energy transition coincide with the experimentally measured lowest energy naphthyl-centered transition at 279 nm. This transition is chosen as the reference energy since all *S*-calixarenes possess positive transitions of similar magnitudes (within a factor of 2 per naphthyl group) and nearly identical molar absorptivities at this wavelength. The

Table 3 Experimental absorption and CD spectral properties of **2**, **14**, **6**, *tert*-butylcalix[4]arene in dichloromethane at 25°

		Transitions above 260 nm					
Compound		291 nm	283 nm	279 nm	262 nm	ε_{exp} at λ_{max}	$[\theta]_{exp}$[a] at 279 nm
2	$[\varepsilon]_{fit}$[b]	2.0	5.8	10.8	7.1	17.4 (278)	10 800
14	$[\varepsilon]_{fit}$	2.0	5.8	11.6	6.7	17.8 (277)	5600
6	$[\varepsilon]_{fit}$	2.0	5.8	12.0	3.1	18.5 (278)	3300
tert-Butyl-calixarene	$[\varepsilon]_{fit}$	2.0	5.8	0	0	6.3 (280)	—
1-(α-Naphthyl)ethanol	—	—	—	—	—	—	400[c]

[a] Reported as deg cm^{-2} $dmol^{-1}$ measured from 0.2 mM solution. [b] Reported as $M^{-1} \times 10^{-3}$ measured from 0.05 mM solution. [c] Reported at 275 nm.

correspondence of sign and overall curve shape between simulated and experimental spectra strongly suggests that the simulations of the model accurately capture the local effects of the absolute configuration at the chiral carbon in the calixarenes.

The calculated individual transitions in the simulated CD spectra of 1-(α-naphthyl)ethanol are weak, as observed experimentally, and depend strongly on the chosen dihedral angle, further suggesting that the strong CD spectra observed experimentally for the substituted calixarenes are due to unique interactions between the π systems of the calixarenes and the chiral pendant group. Further examination of the molecular orbitals responsible for the optically active transitions in **16** shows a predominantly naphthyl π and π* character of molecular orbitals that contribute to the lowest energy naphthyl transition, with additional contributions from orbitals delocalized over the entire molecule **16**. The contribution of these orbitals to the optically active transitions explains the inability of this molecular model to accurately capture transitions due to the calixarene macrocycle appearing at 283 nm and 291 nm. Experimentally, the sign and magnitude of optically-active transitions inherent to the calixarene macrocycle (283 nm and 291 nm) are extremely sensitive to the rigidity, and therefore dynamic conformation, of the calixarene (*e.g.* **2** *versus* **14** in Fig. 5 *versus* S30 in ESI†), as are magnitudes of diastereotopic chemical shift differences, measured for calixarene compounds *via* ^{1}H NMR spectroscopy, as discussed above.

Conclusions

The efficient synthesis of a family of chiral calixarene ligands possessing asymmetric centers directly attached to the lower rim is described. The highly stereoselective synthetic approach relies on the Mitsunobu protocol and functions according to S_N2 mechanism with full inversion of configuration as demonstrated *via* single-crystal X-ray diffraction and supported by electronic circular dichroism and simulation. This approach allows direct attachment of asymmetric centers having substituents with differing electron donating/withdrawing properties and steric bulk. The degree of alkylation achieved is highly sensitive to upper-rim substitution pattern and reaction conditions. Induction of asymmetry in this family of ligands is investigated by measuring chemical shift differences for resonances of diastereotopic *meta* and methylene bridge hydrogens in the products. The large observed chemical shift differences suggest the presence of a highly asymmetric environment encompassing the entire calixarene macrocycle, which is sensitive to the steric bulk and chemical structure of substituents on the asymmetric centers, and demonstrates the importance of conformational rigidity and direct connectivity between lower rim oxygens and asymmetric centers for efficient induction of asymmetry throughout the entire calixarene scaffold. DFT-based calculations support trends observed experimentally *via* NMR and CD spectroscopies. The subsequent metallation of these ligands and their grafting onto solid supports will be reported in due course.

Experimental section

All compounds were handled using Schlenk techniques under dry nitrogen atmosphere. Solvents were dried and distilled by standard methods. Starting *p-tert*-butylcalix[4]arene and all others reagents were of analytical grade and used as received. All chiral alcohols were commercially available with the exception of the *trans*-1-*N*-Cbz-aminocyclopentanol. This latter compound was synthesized by treating the commercially available free *trans*-aminopentanol hydrochloride (0.5 g, 3.63 mmol) with benzyl chloroformate (0.93 g, 5.45 mmol) and sodium bicarbonate (0.61 g, 7.26 mmol) in 5 : 1 water–THF as solvent at room temperature and stirring for 40 min (yield 59%). ^{1}H and ^{13}C NMR spectra were recorded in $CDCl_3$ (293 K) either on a Bruker AV-300 (300 MHz) instrument or on a AVB-400 (400 MHz) instrument, and 2D COSY and 1D NMR were performed on DRX-500 (500 MHz) instrument at the UC Berkeley NMR Facility. The ^{1}H NMR data are referenced to residual $CHCl_3$ (7.26 ppm) and ^{19}F NMR data are referenced relative to $CFCl_3$. Analytical thin-layer chromatography was performed on precoated silica gel plates (0.25 mm, 60F-254, Merck), and silica gel (Selecto 60) was used for column chromatography. Diastereoselectivity was measured by HPLC-MS with an Agilent 1100 LS-MS system equipped with a Daicel CHIRACEL OD column monitored at 210 and 254 nm. Optical rotations were measured on a Perkin-Elmer Model 241 polarimeter. FAB-MS spectra were recorded with using *o*-nitrophenyl octyl ether (NPOE) as matrix at the UC Berkeley Mass Spectrometry Facility. All melting points are uncorrected.

CD and UV-Vis spectroscopy

UV-visible spectra of 0.05 mM solutions in dichloromethane were collected in standard 1 cm pathlength quartz cells at room temperature using a Cary 400 Bio UV-visible spectrophotometer. Spectra were collected with a 0.5 nm interval and a dwell time of 0.1 s. Circular dichroism spectra of 0.2 mM solutions in dichloromethane were collected in standard 1 cm pathlength quartz cells at room temperature using a Jasco J-810 spectropolarimeter. Spectra were collected at 10 nm min^{-1} with an 8 s response time, and a 0.2 nm pitch width. Data were averaged over 2–6 acquisitions and noise reduced using a one-pass fast Fourier transform.

Ab initio modeling of CD spectrum

Molecular fragment optimizations were performed at the DFT/B3LYP/6-31+G* level of theory using the Gaussian03 software package.[35] Electronic transitions (UV and CD) were also simulated with Gaussian 03 software using the TD-DFT approach, the B3LYP functional and the 6-31+G* basis, but simulated spectra were nearly identical employing 6-31G* as basis. In this report, rotary strengths are given in the dipole length formalism (R^r), which was reported to be more robust,[34] but results using the velocity formalism were similar. The experimental spectra were simulated by broadening the simulated rotary strengths according to the equation:

$$\Delta\varepsilon(E) = \frac{\sum_{i=1}^{n} \Delta E_i R_i e^{-\left[\frac{(E-\Delta E_i)}{2\sigma}\right]^2}}{2.297 \times 10^{-39}\sqrt{2\pi\sigma}}$$

where σ is the width of the band width, chosen to be 0.15 eV as an empirical parameter to give good visual agreement with the

experimental data; ΔE_i and R_i are the excitation energies and rotational strengths for transition i as simulated. Ten transitions were determined for each molecular fragment, but generally four or fewer fell in the relevant energy range. TDDFT/B3LYP have been shown to underestimate energies,[34] so simulated transitions were shifted to match the experimental CD maxima. The lack of relevant Rydberg states or double and higher excitations in the energy range of the experimental spectra suggests that there will be good agreement between the experimental spectra recorded in dichloromethane and the simulated spectra. In general, it has been previously found that TD-DFT used with this functional can be used to assign absolute configurations of chiral molecules with high certainty.[34]

Conformational searches were performed using MacroModel 9.1 and an MMFF force field in gas phase. All torsional angles between the naphthalene fragment and the calixarene [C(calixarene)–O–CH(CH_3)–C(naphthalene)] and the calixarene phenol torsional angles were subject to a Monte Carlo random walk algorithm.

Calculated ^{1}H NMR chemical shifts

^{1}H NMR chemical shifts were calculated for **2**, **4**, **7** and **8**. In each case, the lowest energy conformations were identified using a Monte Carlo conformational search using the OPLS2006 force field in MacroModel 9.1 as implemented in Maestro 6.5. These structures were further optimized at B3LYP/6-31G** and then single point calculations at B3LYP/6-311G**++ were performed to determine the shielding constants. This level of theory has been shown to give good correlation with experimental chemical shifts.[36] Because of the large size of the molecules, the pseudospectral_DFT method implemented in Jaguar 6.5 was used. This is a GIAO (gauge-including atomic orbitals) based approach shown to give good results for organic molecules.[37]

Crystallography

The crystal structures of **2** and **7** were determined by single crystal X-ray diffraction. Data measurements were made on a Bruker APEX[38] CCD area detector with graphite monochromated Mo-Kα radiation. The structure was solved by direct methods[39] and expanded using Fourier techniques.[40] Neutral atom scattering factors were taken from Cromer and Waber.[41] Anomalous dispersion effects were included in F_{calc};[42] the values for $\Delta f'$ and $\Delta f''$ were those of Creagh and McAuley.[43] The values for the mass attenuation coefficients are those of Creagh and Hubbel.[44] All calculations were performed using the teXsan[45] crystallographic software package of Molecular Structure Corporation.

Crystal data and refinement details for 2. $C_{70}O_4H_{77}N$, M_r = 996.38, monoclinic, space group $P2_1$, a = 12.305(1), b = 12.911(1), c = 19.409(2) Å, V = 2970.3(5) Å^3, Z = 2, D_c = 1.11 g cm^{-3}, μ = 0.67 cm^{-1}, $F(000)$ = 1072.00. No. of reflections measured – total: 12 298, unique: 3658 (R_{int} = 0.039), R = 0.083, R_w = 0.088, R_{all} = 0.103, $\Delta\rho_{max}$ = 0.51, $\Delta\rho_{min}$ = −0.27 e Å^{-3}.

Crystal data and refinement details for 7. $C_{78}N_2O_{12}H_{110}$, M_r = 1267.73, monoclinic, space group $P2_1$, a = 13.170(1), b = 19.498(2), c = 14.880(2) Å, V = 3640.3(7) Å^3, Z = 2, D_c = 1.156 g cm^{-3}, μ = 0.76 cm^{-1}, $F(000)$ = 1376.00. No. of reflections measured – total: 20 864, unique: 7784 (R_{int} = 0.044), R = 0.058, R_w = 0.059, R_{all} = 0.090, $\Delta\rho_{max}$ = 0.36, $\Delta\rho_{min}$ = −0.26 e Å^{-3}.

General procedure for chiral HPLC calibration

A control stereoisomeric mixture of **2**, **3**, and related *meso* form was used for chiral HPLC calibration. This mixture was synthesized using a racemic mixture of naphthalenemethanol as reactant under otherwise similar Mitsunobu protocol reaction conditions, described above for dialkylation in Scheme 2. A doubling of all resonances was observed *via* ^{1}H NMR spectroscopy and for carbons close to the chiral center *via* ^{13}C NMR spectroscopy, including the chiral methylene carbon C*H (84.36 and 84.29 ppm) and methyl CH_3C*H (21.88 and 22.10 ppm), due to the presence of the magnetically inequivalent *meso*-(*R*,*S*) form. The lower symmetry of the *meso*-(*R*,*S*) form led to characteristic *tert*-butyl resonances at 0.92 ppm, 1.14 ppm, and 1.32 ppm in a ratio of 18H : 9H : 9H.

General procedure for the synthesis of calixarenes 1–6 and 8–13 *via* Mitsunobu reaction

To a mixture of parent calix[4]arene (0.154 mmol) and chiral alcohol (0.77 mmol) in 5 ml of THF (benzene for synthesis of **10**), triphenylphosphine (0.46 mmol for synthesis of **1–4**, **8**, **10**, **11**, **12** and 0.23 mmol for synthesis of **5, 6**, **9**, **10**, **13**) was added. The resulting mixture was cooled to 0 °C, and diethyl azodicarboxylate (0.46 mmol for synthesis of **1–4**, **8**, **10**, **11**, **12** 0.23 mmol for synthesis of **5, 6**, **9**, **10**, **13**) was added dropwise as a 40% solution in toluene. After 10 min of stirring, a colored solution formed, which was heated to room temperature. After 24 h of stirring at room temperature (for the synthesis of **8**, the reaction was stopped after 8 h as well as after 24 h), and the solution was evaporated to dryness. The residue was treated with 2 mL of methanol for 20 min at room temperature, followed by evaporation to dryness. Compounds **1–6** and **8–13** were subsequently purified using column chromatography.

5,11,17,23-Tetra-*tert*-butyl-25,27-bis[(*S*)-1-phenylethoxy]-26,28-dihydroxy-calix[4]arene (1). Column chromatography with CH_2Cl_2–*n*-hexane (1 : 1) afforded 60% of white powder: mp 134–133 °C; $[\alpha]_D^{21}$ = −23 (*c* 0.70, CH_2Cl_2); ^{1}H NMR (300 MHz, $CDCl_3$) δ 7.58 (d, ^3J = 6.6 Hz, 4H, C_6H_5), 7.32–7.42 (m, 6H, C_6H_5), 7.21 (s, 2H, OH), 7.04 (d, ^4J = 2.4 Hz, 2H, ArH-*m*), 6.89 (d, ^4J = 2.4 Hz, 2H, ArH-*m*), 6.80 (d, ^4J = 2.4 Hz, 2H, ArH-*m*), 6.68 (d, ^4J = 2.4 Hz, 2H, ArH-*m*), 5.00 (q, ^3J = 6.6 Hz, 2H, C*H*CH_3), 4.53 (d, ^2J = 12.9 Hz, 2H, ArCH_2-Ar), 3.82 (d, ^2J = 13.5 Hz, 2H, ArCH_2Ar), 3.29 (d, ^2J = 12.9 Hz, 2H, ArCH_2Ar), 2.94 (d, ^2J = 13.5 Hz, 2H, ArCH_2Ar), 1.78 (d, ^3J = 6.6 Hz, 6H, CHC*H*$_3$), 1.25 (s, 18H, C(CH_3)$_3$), 0.93 (s, 18H, C(CH_3)$_3$); elemental analysis calcd (%) for $C_{60}H_{72}O_4$: C 84.07, H 8.47; found C 84.02, H 8.65; HR FAB MS calcd for $C_{60}H_{72}O_4$ 856.543061, found 856.541400.

5,11,17,23-Tetra-*tert*-butyl-25,27-bis[(*S*)-α-methyl-2-naphthalenemethoxy]-26,28-dihydroxy-calix[4]arene (2). Column chromatography with CH_2Cl_2–*n*-hexane (0.8 : 1) afforded 75% of white powder: mp 139–141 °C; $[\alpha]_D^{21} = -90$ (*c* 0.70, CH_2Cl_2); ^{1}H NMR (400 MHz, $CDCl_3$) δ 7.80–7.89 (m, 10H, $C_{10}H_7$), 7.44–7.50 (m, 4H, $C_{10}H_7$), 7.30 (s, 2H, OH), 7.05 (d, ^4J = 2.1 Hz, 2H, ArH-*m*), 6.86 (d, ^4J = 2.1 Hz, 2H, ArH-*m*), 6.84 (d, ^4J = 2.4 Hz, 2H, ArH-*m*), 6.66 (d, ^4J = 2.4 Hz, 2H, ArH-*m*), 5.17 (q, ^3J = 6.4 Hz, 2H, C*H*CH_3), 4.58 (d, ^2J = 12.8 Hz, 2H, $ArCH_2Ar$), 3.89 (d, ^2J = 13.2 Hz, 2H, $ArCH_2Ar$), 3.35 (d, ^2J = 12.8 Hz, 2H, $ArCH_2Ar$), 2.85 (d, ^2J = 13.6 Hz, 2H, $ArCH_2Ar$), 1.90 (d, ^3J = 6.4 Hz, 6H, CHCH_3), 1.24 (s, 18H, $C(CH_3)_3$), 0.94 (s, 18H, $C(CH_3)_3$); ^{13}C NMR (400 MHz, $CDCl_3$) δ 150.84, 148.83, 146.49, 141.16, 139.28, 133.19, 132.86, 128.22, 127.73, 127.54, 125.94, 125.58, 125.32, 124.99, 124.92, 124.79, 84.34, 33.90, 33.77, 32.23, 31.70, 31.04, 21.90; elemental analysis calcd (%) for $C_{68}H_{76}O_4$: C 85.31, H 8.00; found C 85.00, H 8.10; HR FAB MS calcd for $C_{68}H_{75}O_4$ 955.566537, found 955.568630.

5,11,17,23-Tetra-*tert*-butyl-25,27-bis[(*R*)-α-methyl-2-naphthalenemethoxy]-26,28-dihydroxy-calix[4]arene (3). Column chromatography with CH_2Cl_2–*n*-hexane (0.8 : 1) afforded 70% yield of white powder: mp 139–141 °C; $[\alpha]_D^{21} = +88$ (*c* 0.70, CH_2Cl_2); ^{1}H NMR (500 MHz, $CDCl_3$) δ 7.79–7.88 (m, 10H, $C_{10}H_7$), 7.94 (m, 4H, $C_{10}H_7$), 7.31 (s, 2H, OH), 7.05 (d, ^4J = 2.5 Hz, 2H, ArH-*m*), 6.85 (d, ^4J = 2.5 Hz, 2H, ArH-*m*), 6.83 (d, ^4J = 2.5 Hz, 2H, ArH-*m*), 6.65 (d, ^4J = 2.5 Hz, 2H, ArH-*m*), 5.16 (q, ^3J = 6.5 Hz, 2H, C*H*CH_3), 4.57 (d, ^2J = 13.0 Hz, 2H, $ArCH_2Ar$), 3.88 (d, ^2J = 13.0 Hz, 2H, $ArCH_2Ar$), 3.35 (d, ^2J = 13.0 Hz, 2H, $ArCH_2Ar$), 2.84 (d, ^2J = 13.5 Hz, 2H, $ArCH_2Ar$), 1.89 (d, ^3J = 6.5 Hz, 6H, CHCH_3), 1.23 (s, 18H, $C(CH_3)_3$), 0.94 (s, 18H, $C(CH_3)_3$); elemental analysis calcd (%) for $C_{68}H_{76}O_4$: C 85.31, H 8.00; found C 85.03, H 8.08; HR FAB MS calcd for $C_{68}H_{75}O_4$ 955.566537, found 955.568060.

5,11,17,23-Tetra-*tert*-butyl-25,27-bis[(*S*)-α-trifluoromethyl-1-phenylmethoxy]-26,28-dihydroxy-calix[4]arene (4). Column chromatography with CH_2Cl_2–*n*-hexane (0.5 : 1) afforded 60% yield of white powder: mp 137–140 °C; $[\alpha]_D^{23} = -38$ (*c* 0.70, CH_2Cl_2); ^{1}H NMR (400 MHz, $CDCl_3$) δ 7.74 (d, ^3J = 6.8 Hz, 4H, $C_{10}H_7$), 7.46–7.54 (m, 6H, $C_{10}H_7$), 7.05 (d, ^4J = 2.4 Hz, 2H, ArH-*m*), 6.97 (d, ^4J = 2.4 Hz, 2H, ArH-*m*), 6.63 (m, 4H, ArH-*m*), 5.68 (s, 2H, OH), 5.13 (m, 2H, C*H*CH_3), 4.49 (d, ^2J = 13.6 Hz, 2H, $ArCH_2Ar$), 3.78 (d, ^2J = 13.2 Hz, 2H, $ArCH_2Ar$), 3.32 (d, ^2J = 13.6 Hz, 2H, $ArCH_2Ar$), 3.10 (d, ^2J = 13.2 Hz, 2H, $ArCH_2Ar$), 1.27 (s, 18H, $C(CH_3)_3$), 0.83 (s, 18H, $C(CH_3)_3$); ^{19}FNMδ −73.74 (d, 3.76 Hz); ^{13}C NMR (500 MHz) δ 150.29, 150.16, 147.10, 132.07, 130.71, 129.84, 128.50, 128.17, 128.02, 127.55, 125.99, 125.41, 125.10, 124.64, 83.88, 33.77, 33.73, 31.79, 31.62, 30.77; elemental analysis calcd (%) for $C_{60}H_{66}F_6O_4$: C 74.67, H 6.89; found C 74.64, H 6.59; FAB MS calcd for $C_{60}H_{66}O_4F_6$ 964.486531, found 964.485880.

5,11,17,23-Tetra-*tert*-butyl-25-(*S*)-1-phenylethoxy-26,27,28-trihydroxy-calix[4]arene (5). Column chromatography with CH_2Cl_2–*n*-hexane (1 : 0.5) afforded 47% yield of white powder: mp 130–132 °C; $[\alpha]_D^{23} = -62$ (*c* 0.70, CH_2Cl_2); ^{1}H NMR (500 MHz, $CDCl_3$) δ 10.14 (s, 1H, OH), 9.60 (s, 1H, OH), 9.31 (s, 1H, OH), 7.48–7.49 (m, 2H, C_6H_5), 7.39 (m, 3H, C_6H_5), 7.19 (d, ^4J = 2.5 Hz, 1H, ArH-*m*), 7.11 (d, ^4J = 2.5 Hz, 1H, ArH-*m*), 7.07 (d, ^4J = 2.0 Hz, 1H, ArH-*m*), 7.01 (d, ^4J = 2.0 Hz, 1H, ArH-*m*), 6.97 (d, ^4J = 2.5 Hz, 1H, ArH-*m*), 6.95 (d, ^4J = 2.5 Hz, 1H, ArH-*m*), 6.90 (d, ^4J = 2.5 Hz, 1H, ArH-*m*), 6.88 (d, ^4J =2.0 Hz, 1H, ArH-*m*), 5.14 (q, ^3J = 6.5 Hz, 1H, C*H*CH_3), 4.73 (d, ^2J = 12.5 Hz, 1H, $ArCH_2Ar$), 4.32 (d, ^2J = 13.5 Hz, 1H, $ArCH_2Ar$), 4.19 (d, ^2J = 13.5 Hz, 1H, $ArCH_2$-Ar), 3.56 (d, ^2J = 13.5 Hz, 1H, $ArCH_2Ar$), 3.46 (d, ^2J = 12.5 Hz, 1H, $ArCH_2Ar$), 3.44 (d, ^2J = 13.5 Hz, 1H, $ArCH_2Ar$), 3.40 (d, ^2J = 13.5 Hz, 1H, $ArCH_2Ar$), 2.92 (d, ^2J = 13.5 Hz, 1H, $ArCH_2Ar$), 2.04 (d, ^3J = 6.5 Hz, 3H, CH_3CH), 1.22 (s, 9H, $C(CH_3)_3$), 1.22 (s, 9H, $C(CH_3)_3$), 1.19 (s, 9H, $C(CH_3)_3$), 1.18 (s, 9H, $C(CH_3)_3$); ^{13}C NMR (500 MHz, $CDCl_3$) δ 149.12, 148.24, 147.87, 147.73, 143.65, 143.22, 142.74, 140.14, 134.87, 133.46, 129.02, 128.80, 128.63, 127.82, 127.74, 127.57, 127.53, 127.26, 126.97, 125.98, 125.83, 125.79, 125.67, 125.55, 125.51, 125.46, 85.50, 34.21, 34.03, 33.92, 33.89, 33.16, 32.95, 32.75, 32.30, 31.64, 31.56, 31.50, 31.27, 22.70, 20.93, 14.16; elemental analysis calcd (%) for $C_{52}H_{64}O_4$: C 82.94, H 8.57; found C 82.89, H 8.36; HR FAB MS calcd for $C_{52}H_{63}O_4$ 751.472636, found 751.473240.

5,11,17,23-Tetra-*tert*-butyl-25-[(*S*)-α-methyl-2-naphthalenemethoxy]-26,27,28-trihydroxy-calix[4]arene (6). Column chromatography with CH_2Cl_2–*n*-hexane (1 : 0.6) afforded 44% yield of white powder: mp 139–142 °C; $[\alpha]_D^{21} = -67$ (*c* 0.70, CH_2Cl_2); ^{1}H NMR (500 MHz, $CDCl_3$) δ 10.16 (s, 1H, OH), 9.65 (s, 1H, OH), 9.38 (s, 1H, OH), 7.92 (d, ^3J = 8.5 Hz, 1H, $C_{10}H_7$), 7.87–7.88 (m, 1H, $C_{10}H_7$), 7.80–7.82 (m, 1H, $C_{10}H_7$), 7.78 (d, ^3J = 8.5 Hz, 1H, $C_{10}H_7$), 7.76 (s, 1H, $C_{10}H_7$), 7.48–7.53 (m, 2H, $C_{10}H_7$), 7.21 (d, ^4J = 2.5 Hz, 1H, ArH-*m*), 7.13 (d, ^4J = 2.5 Hz, 1H, ArH-*m*), 7.07 (d, ^4J = 2.5 Hz, 1H, ArH-*m*), 7.00 (d, ^4J = 2.0 Hz, 1H, ArH-*m*), 6.96 (d, ^4J = 2.5 Hz, 1H, ArH-*m*), 6.95 (d, ^4J = 2.0 Hz, 1H, ArH-*m*), 6.83 (d, ^4J = 2.0 Hz, 2H, ArH-*m*), 5.30 (q, ^3J = 6.0 Hz, 1H, CH_3C*H*), 4.78 (d, ^2J = 13.0 Hz, 1H, $ArCH_2Ar$), 4.34 (d, ^2J = 13.5 Hz, 1H, $ArCH_2Ar$), 4.17 (d, ^2J = 13.5 Hz, 1H, $ArCH_2$-Ar), 3.57 (d, ^2J = 13.5 Hz, 1H, $ArCH_2Ar$), 3.50 (d, ^2J = 13.0 Hz, 1H, $ArCH_2Ar$), 3.45 (d, ^2J = 13.5 Hz, 1H, $ArCH_2Ar$), 3.38 (d, ^2J = 13.5 Hz, 1H, $ArCH_2Ar$), 2.79 (d, ^2J = 13.5 Hz, 1H, $ArCH_2Ar$), 2.13 (d, ^3J = 6.5 Hz, 3H, CH_3CH), 1.22 (s, 9H, $C(CH_3)_3$), 1.22 (s, 9H, $C(CH_3)_3$), 1.18 (s, 9H, $C(CH_3)_3$), 1.14 (s, 9H, $C(CH_3)_3$)); elemental analysis calcd (%) for $C_{56}H_{66}O_4$: C 83.75, H 8.28; found C 83.79, H 8.13; HR FAB MS calcd for $C_{56}H_{65}O_4$ 801.488286, found 801.486660.

5,11,17,23-Tetra-*tert*-butyl-25,27-bis[*cis*-(1*R*,2*S*)-(*N*-benzyloxycarbonyl)-2-aminocyclopentyloxy]-26,28-dihydroxy-calix[4]arene (7). To a mixture of *tert*-butylcalix[4]arene (0.80 g, 1.24 mmol), triphenylphosphine (0.53 g, 1.98 mmol) and DEAD (0.35 g, 1.98 mmol) in 25 ml dry toluene, a solution of *trans*-*N*-benzyloxycarbonylaminocyclopentanol (0.35 g, 1.49 mmol) in 5 ml of dry toluene was added dropwise at 40 °C. The resulting yellow solution was heated at 80 °C for 2 h. The reaction was continued additional 24 h at room temperature. The reaction mixture was evaporated to dryness and purified by column chromatography (DCM–methanol 1 : 0.010 v/v), R_f 0.3. Recrystallization from ethanol afforded

8% of white powder: mp 174–179 °C; ^{1}H NMR (500 MHz, $CDCl_3$) δ 7.43 (d, J = 9.0 Hz, 2H), 7.14–7.16 (m, 4H), 7.05–7.10 (m, 6H, ArH), 7.00–7.02 (m, 4H), 6.84 (s, 2H), 6.73 (s, 2H), 6.63 (s, 2H), 5.19 (d, J = 12.5 Hz, 2H), 4.90 (d, J = 12.5 Hz, 2H), 4.36–4.41 (m, 4H), 4.22 (m, 2H), 3.95 (d, J = 13.5 Hz, 2H), 3.36 (d, J = 13.5, 2H), 3.25 (d, J = 13.0 Hz, 2H), 2.05 (m, 2H), 1.90 (m, 4H), 1.46 (m, 6H), 1.21 (s, 18H), 0.91 (s, 18H). ^{13}C NMR δ 156.99, 150.12, 147.74, 147.34, 142.62, 137.16, 133.35, 132.06, 128.41, 127.52, 127.24, 125.93, 124.96, 89.14, 66.35, 55.86, 34.17, 32.48, 32.00, 31.16, 29.89, 28.20, 19.80; elemental analysis calcd (%) for $C_{70}H_{86}N_2O_8$: C 77.60, H 8.00, N 2.59; found C 77.67, H 8.10, N 2.57; FAB MS calcd for $C_{70}H_{87}N_2O_8$ 1083.646244, found 1083.647670.

5,11,17,23-Tetra-*tert*-butyl-25,27-bis[(*R*)-2-phenyl-1-propoxy]-26,28-dihydroxy-calix[4]arene (8). Column chromatography with CH_2Cl_2–*n*-hexane (0.8 : 1) afforded 80% yield (for the reaction that involved 14 h of stirring) of white powder: mp 164–166 °C; $[\alpha]_D^{21}$ = −20 (*c* 0.70, CH_2Cl_2); ^{1}H NMR (400 MHz, $CDCl_3$) δ 7.50 (s, 2H, OH), 7.38 (d, ^3J = 7.2 Hz, 4H, $C_{10}H_7$), 7.32 (t, ^3J = 7.2 Hz, 4H, $C_{10}H_7$), 7.16 (t, ^3J = 7.2 Hz, 2H, $C_{10}H_7$), 7.06 (d, ^4J = 2.4 Hz, 2H, ArH-*m*), 7.01 (d, ^4J = 2.4 Hz, 2H, ArH-*m*), 6.79 (d, ^4J = 2.4 Hz, 2H, ArH-*m*), 6.81 (d, ^4J = 2.4 Hz, 2H, ArH-*m*), 4.35 (d, ^2J = 12.8 Hz, 2H, $ArCH_2Ar$), 4.15 (d, ^2J = 13.2 Hz, 2H, $ArCH_2Ar$), 4.01 (m, 4H, OCH_2), 3.52 (m, 2H, C*H*CH_3), 3.30 (d, ^2J = 13.2 Hz, 2H, $ArCH_2Ar$), 3.25 (d, ^2J = 12.8 Hz, 2H, $ArCH_2Ar$), 1.79 (d, ^3J = 6.8 Hz, 6H, CHC*H*$_3$), 1.28 (s, 18H, $C(CH_3)_3$), 0.94 (s, 18H, $C(CH_3)_3$); elemental analysis calcd (%) for $C_{62}H_{76}O_4$: C 84.12, H 8.65; found C 84.23, H 8.38; HRMS calcd for $C_{62}H_{76}O_4$ 884.574362, found 884.575380.

5,11,17,23-Tetra-*tert*-butyl-25-(*R*)-2-phenyl-1-propoxy-26,27,28-trihydroxy-calix[4]arene (9). Column chromatography with CH_2Cl_2–*n*-hexane (0.8 : 1) afforded 42% yield (69% in mixture of **8** and **9**) of white powder: mp 173–174 °C; $[\alpha]_D^{21}$ = −24 (*c* 0.70, CH_2Cl_2); ^{1}H NMR (500 MHz, $CDCl_3$) δ 9.95 (s, 1H, OH), 9.28 (s, 1H, OH), 9.15 (s, 1H, OH), 7.49 (d, ^3J = 7.5 Hz, 2H, C_6H_5), 7.43 (t, ^3J = 7.5 Hz, 2H, C_6H_5), 7.30 (t, ^3J = 7.5 Hz, 1H, C_6H_5), 7.12 (d, ^4J = 2.0 Hz, 1H, ArH-*m*), 7.09 (d, ^4J = 2.0 Hz, 1H, ArH-*m*), 7.07 (d, ^4J = 2.0 Hz, 1H, ArH-*m*), 7.04 (d, ^4J = 2.0 Hz, 1H, ArH-*m*), 7.03 (d, ^4J = 2.0 Hz, 1H, ArH-*m*), 7.02 (d, ^4J = 2.0 Hz, 1H, ArH-*m*), 6.99 (d, ^4J = 2.0 Hz, 1H, ArH-*m*), 6.98 (d, ^4J = 2.0 Hz, 1H, ArH-*m*), 4.48 (d, ^2J = 12.5 Hz, 1H, $ArCH_2Ar$), 4.31 (d, ^2J = 13.5 Hz, 1H, $ArCH_2Ar$), 4.20, 4.26 (2 m, 1H each, OCH_2CH), 4.13 (d, ^2J = 13.5 Hz, 1H, $ArCH_2Ar$), 4.10 (d, ^2J = 13.5 Hz, 1H, $ArCH_2Ar$), 3.75 (m, 1H, OCH_2CH), 3.45 (d, ^2J = 13.5 Hz, 1H, $ArCH_2Ar$), 3.41 (d, ^2J = 13.5 Hz, 2H, $ArCH_2Ar$), 3.39 (d, ^2J = 12.5 Hz, 1H, $ArCH_2Ar$), 1.64 (d, ^3J = 6.5 Hz, 3H, CHC*H*$_3$), 1.24 (s, 9H, $C(CH_3)_3$), 1.23 (s, 9H, $C(CH_3)_3$), 1.22 (s, 9H, $C(CH_3)_3$), 1.19 (s, 9H, $C(CH_3)_3$); elemental analysis calcd (%) for $C_{53}H_{66}O_4$: C 82.99, H 8.67; found C 82.91, H 8.73; HR FAB MS calcd for $C_{53}H_{66}O_4$ 766.496111, found 766.497910.

25-(*S*)-α-Methyl-2-naphthalenemethoxy-26,27,28-trihydroxy-calix[4]arene (10). Column chromatography with CH_2Cl_2–*n*-hexane (1 : 0.5) afforded 55% yield (for reaction in benzene) of white powder: mp 115–117 °C; $[\alpha]_D^{21}$ = −53 (*c* 0.70, CH_2Cl_2); ^{1}H NMR (500 MHz, $CDCl_3$) δ 9.65 (s, 1H, OH), 9.31 (s, 1H, OH), 9.25 (s, 1H, OH), 7.94 (d, ^3J = 8.5 Hz, 1H, $C_{10}H_7$), 7.85–7.89 (m, 2H, $C_{10}H_7$), 7.82 (s, 1H, $C_{10}H_7$), 7.78 (d, ^3J = 8.5 Hz, 1H, $C_{10}H_7$), 7.50–7.52 (m, 2H, $C_{10}H_7$), 7.16 (dd, ^3J = 7.5 Hz, ^4J = 2.0 Hz, 1H, ArH-*m*), 7.11 (dd, ^3J = 7.5 Hz, ^4J = 2.0 Hz, 1H, ArH-*m*), 7.00 (dd, ^3J = 7.5 Hz, ^4J = 2.0 Hz, 2H, ArH-*m*), 6.94 (m, 2H, ArH-*m*), 6.81–6.84 (m, 2H + 1H, ArH-*m* + ArH-*p*), 6.66 (t, ^3J = 7.5 Hz, 2H, ArH-*p*), 6.57 (t, ^3J = 7.5 Hz, 1H, ArH-*p*), 5.34 (m, 1H, C*H*CH_3), 4.76 (d, ^2J = 13.0 Hz, 1H, $ArCH_2Ar$), 4.33 (d, ^2J = 13.5 Hz, 1H, $ArCH_2$-Ar), 4.15 (d, ^2J = 13.5 Hz, 1H, $ArCH_2Ar$), 3.67 (d, ^2J = 13.5 Hz, $ArCH_2Ar$), 3.54 (d, ^2J = 13.0 Hz, 1H, $ArCH_2Ar$), 3.47 (d, ^2J = 13.5 Hz, 1H, $ArCH_2Ar$), 3.39 (d, ^2J = 13.5 Hz, 1H, $ArCH_2Ar$), 2.86 (d, ^2J = 13.0 Hz, 1H, $ArCH_2Ar$), 2.10 (d, ^3J = 6.5 Hz, 3H, CHC*H*$_3$); elemental analysis calcd (%) for $C_{40}H_{34}O_4$: C 83.02, H 5.92; found C 83.11, H 5.88; HR FAB MS calcd for $C_{40}H_{34}O_4$ 578.245710, found 578.247470.

25,27-Bis[(*S*)-α-methyl-2-naphthalenemethoxy]-26,28-dihydroxy-calix[4]arene (11). Column chromatography with CH_2Cl_2–*n*-hexane (1 : 0.7) afforded 30% yield of white powder: mp 107–109 °C; $[\alpha]_D^{21}$ = −50 (*c* 0.70, CH_2Cl_2); ^{1}H NMR (400 MHz, $CDCl_3$) δ 7.78–7.91 (m, 10H + 2H, $C_{10}H_7$ + OH), 7.46–7.51 (m, 4H, $C_{10}H_7$), 7.05 (d, ^3J = 7.2 Hz, 2H, ArH-*m*), 6.93 (dd, ^3J = 7.2 Hz, ^4J = 2.0 Hz, 2H, ArH-*m*), 6.84 (d, ^3J = 7.6 Hz, 2H, ArH-*m*), 6.73 (dd, ^3J = 7.6 Hz, ^4J = 2.0 Hz, 2H, J 7.6 Hz, ArH), 6.71 (t, ^3J = 7.6 Hz, 2H, ArH-*p*), 6.57 (t, ^3J = 7.2 Hz, 2H, ArH-*p*), 5.20 (q, ^3J = 6.4 Hz, 2H, CH_3CH), 4.60 (d, ^2J = 12.8 Hz, 2H, $ArCH_2Ar$), 3.85 (d, ^2J = 13.6 Hz, 2H, $ArCH_2Ar$), 3.41 (d, ^2J = 12.8 Hz, 2H, $ArCH_2Ar$), 2.87 (d, ^2J = 13.6 Hz, 2H, $ArCH_2Ar$), 1.93 (d, ^3J = 6.4 Hz, 6H, CHC*H*$_3$); elemental analysis calcd (%) for $C_{52}H_{44}O_4$: C 85.22, H 6.05; found C 85.39, H 6.19; HRMS calcd for $C_{52}H_{44}O_4$ 732.323960, found 732.323140.

25,27-Bis[(*S*)-1-phenylethoxy]-26,28-dihydroxy-calix[4]arene (12). Column chromatography with CH_2Cl_2–*n*-hexane (1 : 0.6) afforded 42% yield of white powder: mp 132–133 °C, $[\alpha]_D^{21}$ = −71 (*c* 0.70, CH_2Cl_2); ^{1}H NMR (500 MHz, $CDCl_3$) δ 7.86 (s, 2H, OH), 7.55 (d, ^3J = 7.0 Hz, 4H, C_6H_5), 7.34–7.41 (m, 6H, C_6H_5), 7.05 (d, ^3J = 7.0 Hz, 2H, ArH-*m*), 6.92 (d, ^3J = 7.5 Hz, 2H, ArH-*m*), 6.88 (d, ^3J = 7.0 Hz, 2H, ArH-*m*), 6.76 (d, ^3J = 7.5 Hz, 2H, ArH-*m*), 6.70 (t, ^3J = 7.5 Hz, 2H, ArH-*p*), 6.58 (t, ^3J = 7.0 Hz, 2H, ArH-*p*), 5.03 (q, ^3J = 6.5 Hz, 2H, CH_3CH), 4.56 (d, ^2J = 12.5 Hz, 2H, $ArCH_2Ar$), 3.78 (d, ^2J = 13.5 Hz, 2H, $ArCH_2Ar$), 3.38 (d, ^2J = 12.5 Hz, 2H, $ArCH_2$-Ar), 2.94 (d, ^2J = 13.5 Hz, 2H, $ArCH_2Ar$), 1.86 (d, ^3J = 6.5 Hz, 6H, CHC*H*$_3$); elemental analysis calcd (%) for $C_{44}H_{40}O_4$: C 83.52, H 6.37; found C 83.64, H 6.48; HR FAB MS calcd for $C_{44}H_{40}O_4$ 632.292660, found 632.292000.

25-(*S*)-1-Phenylethoxy,26,27,28-trihydroxy-calix[4]arene (13). Column chromatography with CH_2Cl_2–*n*-hexane (1 : 0.6) afforded 47% yield of white powder: mp 144–145 °C, $[\alpha]_D^{21}$ = −68 (*c* 0.70, CH_2Cl_2); ^{1}H NMR (500 MHz, $CDCl_3$) δ 9.66 (s, 1H, OH), 9.28 (s, 1H, OH), 9.21 (s, 1H, OH), 7.48 (m, 2H, C_6H_5), 7.39 (m, 3H, C_6H_5), 7.14 (d, ^3J = 7.5 Hz, 1H, ArH-*m*), 7.09 (d, ^3J = 7.5 Hz, 1H, ArH-*m*), 6.94–7.00 (m, 4H, ArH-*m*), 6.87 (m, 2H, ArH-*m*), 6.82 (t, ^3J = 7.5 Hz, 1H, ArH-*p*), 6.66 (t, ^3J = 7.5 Hz, 1H, ArH-*p*), 6.65 (t, ^3J = 7.5 Hz, 1H, ArH-*p*), 6.60 (t, ^3J = 7.5 Hz, 1H, ArH-*p*), 5.17 (q, ^3J = 7.0 Hz,

1H, CH_3CH), 4.70 (d, ^2J = 12.5 Hz, 1H, $ArCH_2Ar$), 4.30 (d, ^2J = 13.5 Hz, 1H, $ArCH_2Ar$), 4.17 (d, ^2J = 14.0 Hz, 1H, $ArCH_2Ar$), 3.60 (d, ^2J = 13.5 Hz, 1H, $ArCH_2Ar$), 3.50 (d, ^2J = 12.5 Hz, 1H, $ArCH_2Ar$), 3.46 (d, ^2J = 14.0 Hz, 1H, $ArCH_2Ar$), 3.41 (d, ^2J = 13.5 Hz, 1H, $ArCH_2Ar$), 2.92 (d, ^2J = 13.5 Hz, 1H, $ArCH_2Ar$), 2.04 (d, ^3J = 7.0 Hz, 3H, $CHCH_3$); elemental analysis calcd (%) for $C_{36}H_{32}O_4$: C 81.79, H 6.10; found C 81.86, H 6.05; HR FAB MS calcd for $C_{36}H_{32}O_4$ 528.230060, found 528.230560.

5,11,17,23-Tetra-*tert*-butyl-25,27-bis[(*S*)-α-methyl-2-naphthalenemethoxy],26,28-dipropoxy-calix[4]arene (14). To a suspension of sodium hydride (0.1 g, 4 mmol) in 3 ml of DMF, calixarene **1b** (0.2 g, 0.2 mmol) was added, to which *n*-propyl bromide (0.49 g, 4 mmol) was added dropwise. The resulting reaction mixture was stirred at room temperature for 2 h. The white slurry was poured into 25 ml of water and subsequently extracted with 15 mL of $CHCl_3$. The organic solution was evaporated, and the residue was washed with 5 mL of methanol. The resulting white solid was filtered and dried under vacuum. A white powder was obtained in 60% yield; mp 134–136 °C; $[\alpha]_D^{21}$ = −86 (*c* 0.70, CH_2Cl_2); ^{1}H NMR (400 MHz, $CDCl_3$) δ 7.856 (m, 2H, ArH), 7.831 (d, ^3J = 8.8 Hz, 2H, $C_{10}H_7$), 7.768 (m, 2H, $C_{10}H_7$), 7.707 (s, 2H, $C_{10}H_7$), 7.656 (dd, ^3J = 8.4, ^4J = 1.6 Hz, 2H, ArH), 7.430–7.500 (m, 4H, ArH), 7.121 (d, ^4J = 2.4 Hz, 2H, ArH-*m*), 7.004 (d, ^4J = 2.4 Hz, 2H, ArH-*m*), 6.418 (d, ^4J = 2.4 Hz, 2H, ArH-*m*), 6.319 (d, ^4J = 2.4 Hz, 2H, ArH-*m*), 4.758 (q, ^3J = 6.4 Hz, 2H, CH_3CH), 4.591 (d, ^2J = 12.4 Hz, 2H, $ArCH_2Ar$), 4.187 (d, ^2J = 12.4 Hz, 2H, $ArCH_2Ar$), 3.665, 3.793 (2 m, 2H each, OCH_2CH_2), 3.205 (d, ^2J = 12.4 Hz, 2H, $ArCH_2Ar$), 2.733 (d, ^2J = 12.4 Hz, 2H, $ArCH_2Ar$), 1.716 (m, 4H, OCH_2CH_2), 1.612 (d, ^3J = 6.4 Hz, 6H, CH_3CH), 1.326 (s, 18H, $C(CH_3)_3$), 0.803 (s, 18H, $C(CH_3)_3$), 0.351 (t, ^3J = 7.6 Hz, 6H, CH_2CH_3); ^{13}C NMR (400 MHz, $CDCl_3$) δ 154.72, 151.25, 144.39, 143.81, 140.31, 135.81, 133.23, 132.49, 132.19, 128.07, 127.79, 127.67, 126.47, 125.88, 125.77, 125.54, 125.46, 125.34, 124.40, 123.94, 83.57, 34.08, 33.60, 31.81, 31.64, 31.19, 22.89, 21.32, 9.30; elemental analysis calcd (%) for $C_{74}H_{88}O_4$: C 85.34, H 8.52; found C 85.38, H 8.66; FAB MS calcd for $C_{74}H_{88}O_4$ 1040.668262, found 1040.668730.

Acknowledgements

Funding from the US Department of Energy (DE-FG02-05ER15696) and National Science Foundation under the Nanoscale Exploratory Research (NER) program is gratefully acknowledged (CTS 0403710). NSF CHE-0233882 funded the computing equipment used in the computational aspects of this project. The authors would like to thank Dr Frederick Hollander and Dr Allen Oliver of the UC Berkeley CHEXRAY facility for determining the structures of **2** and **7** *via* single crystal X-ray diffraction.

References

1. J. M. Notestein and A. Katz, *Chem.–Eur. J.*, 2006, **12**, 3954–3965.
2. M. Anderson, A. Willetts and S. Allenmark, *J. Org. Chem.*, 1997, **62**, 8455–8458; A. Butler and J. N. Carter-Franklin, *Nat. Prod. Rep.*, 2004, **21**, 180–188; J. N. Carter-Franklin and A. Butler, *J. Am. Chem. Soc.*, 2004, **126**, 15060–15066; M. Andersson and S. Allenmark, *Biocatal. Biotransform.*, 2000, **18**, 79–86; H. B. Brink, A. Tuynman, H. L. Dekker, W. Hemrika, Y. Izumi, T. Oshiro, H. E. Schoemaker and R. Wever, *Inorg. Chem.*, 1998, **37**, 6780–6784; F. Van de Velde, I. W. C. E. Arends and R. A. Sheldon, *J. Inorg. Biochem.*, 2000, **80**, 81–89.
3. J. M. Notestein, E. Iglesia and A. Katz, *J. Am. Chem. Soc.*, 2004, **126**, 16478–16486; J. M. Notestein, L. R. Andrini, V. I. Kalchenko, F. G. Requejo, A. Katz and E. Iglesia, *J. Am. Chem. Soc.*, 2007, **129**, 1122–1131; J. M. Notestein, A. Solovyov, L. R. Andrini, F. G. Requejo, A. Katz and E. Iglesia, *J. Am. Chem. Soc.*, 2007, **129**, 15585–15595; J. M. Notestein, E. Iglesia and A. Katz, *Chem. Mater.*, 2007, **19**, 4998–5005.
4. S. Kobayashi, T. Hamada, S. Nagayama and K. Manabe, *J. Braz. Chem. Soc.*, 2001, **12**, 627–633.
5. D. Meunier, A. Piechaczyk, A. de Mallmann and J.-M. Basset, *Angew. Chem., Int. Ed.*, 1999, **38**, 3540–3542; C. Carlini, E. Chiellini and R. Solaro, *J. Polym. Sci., Polym. Chem. Ed.*, 1980, **18**, 2129–2142; L. H. Gade, P. Renner, H. Memmler, F. Fecher, C. H. Galka, M. Laubender, S. Radojevic, M. McPartlin and J. W. Lauher, *Chem.–Eur. J.*, 2001, **7**, 2563–2580; C. Foltz, M. Enders, S. Bellemin-Laponnaz, H. Wadepohl and L. H. Gade, *Chem.–Eur. J.*, 2007, **13**, 5994–6008; H. Luetjens, G. Wahl, F. Moeller, P. Knochel and Sundermeyer, *Organometallics*, 1997, **16**, 5869–5878; F. Di Furia, G. Licini, G. Modena and R. Motterle, *J. Org. Chem.*, 1996, **61**, 5175–5177; M. G. Finn and B. Sharpless, *J. Am. Chem. Soc.*, 1991, **113**, 113–126.
6. A. Soriente, M. De Rosa, M. Fruilo, L. Lepore, C. Gaeta and P. Neri, *Adv. Synth. Catal.*, 2005, **347**, 816–824.
7. J. Rebek and R. McCready, *J. Am. Chem. Soc.*, 1980, **102**, 5602–5605.
8. W. Shum, R. J. Saxton and J. G. Zajacek, *US Patent* 5663384, 1997.
9. T. P. Yoon and E. N. Jacobsen, *Science*, 2003, **299**, 1691–1693.
10. S. Shinkai, T. Arimura, H. Kawabata, H. Murakami and K. Iwamoto, *J. Chem. Soc., Perkin Trans. 1*, 199110), 2429–2434; G. Ferguson, J. F. Gallagher, L. Giunta, P. Neri, S. Pappalardo and M. Parisi, *J. Org. Chem.*, 1994, **59**, 42–53; Y. Okada, Y. Kasai and J. Nishimura, *Tetrahedron Lett.*, 1995, **36**, 555–557; F. Sansone, S. Barboso, A. Casnati, N. Fabbi, A. Pochini, F. Ugozzoli and R. Ungaro, *Eur. J. Org. Chem.*, 1998, 897–905; V. Boehmer, F. Marschollek and L. Zetta, *J. Org. Chem.*, 1987, **52**, 3200–3205; G. Andreetti, V. Boehmer, J. Graham Jordon, M. Tabatabai, F. Ugozzoli, V. Vogt and A. Wolff, *J. Org. Chem.*, 1993, **58**, 4023–4032; P. Neri, A. Bottino, C. Geraci and M. Piattelli, *Tetrahedron: Asymmetry*, 1996, **7**, 17–20; S. J. Meunier and R. Roy, *Tetrahedron Lett.*, 1996, **37**, 5469–5472; X. Xu, H.-S. Yuan and Z.-T. Huang, *Tetrahedron: Asymmetry*, 1999, **10**, 429–437; A. Soi, J. Pfeiffer, J. Jauch and V. Schurig, *Tetrahedron: Asymmetry*, 1999, **12**, 177–182; J. He, A. S. C. Chan, X. Han and J.-P. Cheng, *Tetrahedron: Asymmetry*, 1999, **10**, 2685–2689; F. Sansone, S. Barboso, A. Casnati, D. Sciotto and R. Ungaro, *Tetrahedron Lett.*, 1999, **40**, 4741–4744; P. Parzuchowski, V. Boehmer, S. Biali and I. Thondorf, *Tetrahedron: Asymmetry*, 2000, **11**, 2393–2402; L. Frkanec, A. Visnjevac, B. Kojic-Prodic and M. Zinic, *Chem.–Eur. J.*, 2000, **6**, 442–453; J. Budka, M. Tkadlecova, P. Lhotak and I. Stibor, *Tetrahedron*, 2000, **56**, 1883–1887; R. E. Brewster and S. B. Shuker, *J. Am. Chem. Soc.*, 2002, **124**, 7902–7903; S. Sdira, C. P. Felix, M.-B. A. Giudicelli, P. F. Seigle-Ferrand, M. Perrin and R. J. Lamartine, *J. Org. Chem.*, 2003, **68**, 6632–6638; A. Casnati, F. Sansone and R. Ungaro, *Acc. Chem. Res.*, 2003, **36**, 246–254; H. Xu, G. R. Kinsel, J. Zhang, M. Li and D. M. Rudkevich, *Tetrahedron*, 2003, **59**, 5837–5848; F. Sansone, L. Baldini, A. Casnati, E. Chierici, G. Faimani, F. Ugozzoli and R. Ungaro, *J. Am. Chem. Soc.*, 2004, **126**, 6204–6205; Y. S. Zheng and C. Zhang, *Org. Lett.*, 2004, **6**, 1189–1192; S. Francese, A. Cozzolino, I. Caputo, C. Esposito, M. Martino, C. Gaeta, F. Troisi and P. Neri, *Tetrahedron Lett.*, 2005, **46**, 1611–1615; C. Gaeta, M. De Rosa, M. Fruilo, A. Soriente and P. Neri, *Tetrahedron: Asymmetry*, 2005, **16**, 2333–2340.
11. W. Verboom, P. J. Bodewes, G. van Essen, P. Timmerman, G. J. van Hummel, S. Harkema and D. N. Reinhoudt,

Tetrahedron, 1995, **51**, 499–512; M. O. Vysotsky, M. O. Tairov, V. V. Pirozhenko and V. I. Kalchenko, *Tetrahedron Lett.*, 1998, **39**, 6057–6060; M. A. Tairov, M. O. Vysotsky, O. I. Kalchenko, V. V. Pirozhenko and V. I. Kalchenko, *J. Chem. Soc., Perkin Trans. 1*, 2002, 1405–1411; Y.-D. Cao, J. Luo, Q.-Y. Zheng, C.-F. Chen, M.-X. Wang and Z.-T. Huang, *J. Org. Chem.*, 2004, **69**, 206–208.
12. R. K. Castellano, B. H. Kim and J. Rebek, Jr, *J. Am. Chem. Soc.*, 1997, **119**, 12671–12672; R. K. Castellano, C. Nuckolls and J. Rebek, Jr, *J. Am. Chem. Soc.*, 1999, **121**, 11156–11163.
13. A. Dondoni, A. Marra, M.-C. Scherrmann, A. Casnati, F. Sansone and R. Ungaro, *Chem.–Eur. J.*, 1997, **3**, 1774–1782.
14. A. Marra, M.-C. Scherrmann, A. Dondoni, A. Casnati, P. Minari and R. Ungaro, *Angew. Chem.*, 1994, **106**, 2533.
15. X. Zeng, L. Weng and Z.-Z. Zhang, *Chem. Lett.*, 2001, **6**, 550–551.
16. A. Ikeda, T. Nagasaki and S. Shinkai, *J. Phys. Org. Chem.*, 1992, **5**, 699–710.
17. J.-B. Regnouf-de-Vains, R. Lamartine and B. Fenet, *Helv. Chim. Acta*, 1998, **81**, 661–669.
18. M. Lazzarotto, F. Nachtigall, I. Vencato and F. Nome, *J. Chem. Soc., Perkin Trans. 2*, 19984), 995–998.
19. J. Wang and C. D. Gutsche, *Struct. Chem.*, 2001, **12**, 267–274.
20. I. Bitter and V. Csokai, *Tetrahedron Lett.*, 2003, **44**, 2261–2265 (31). V. Csokai, A. Grun and I. Bitter, *Tetrahedron Lett.*, 2003, **44**, 4681–4684.
21. V. Csokai, A. Gruen, B. Balazs, G. Toth, G. Horvath and I. Bitter, *Org. Lett.*, 2004, **6**, 477–480.
22. A. Gruen, E. Koszegi and I. Bitter, *Tetrahedron*, 2004, **60**, 5041–5048.
23. V. Csokai, B. Balazs, G. Toth, G. Horvath and I. Bitter, *Tetrahedron*, 2004, **60**, 12059–12066; V. Csokai, A. Simon, B. Balazs, G. Toth and I. Bitter, *Tetrahedron*, 2006, **62**, 2850–2856.
24. S. Shinkai, K. Araki, P. D. J. Grootenhuis and D. N. Reinhoudt, *J. Chem. Soc., Perkin Trans. 2*, 199112), 1883–1886.
25. C. Jaime, J. Mendoza, P. Prados, P. M. Nieto and C. Sanchez, *J. Org. Chem.*, 1991, **56**, 3372–3376.
26. K. Ito, A. Kida, Y. Ohba and T. Sone, *Chem. Lett.*, 1998, **12**, 1221–1222.
27. One of the naphthyl substituents in the X-ray structure is disordered and rotated approximately 180° around its bond with the chiral carbon relative to the other naphthyl substituent on the calixarene. The calixarene exists in a slightly distorted cone conformation in which the substituted phenyl rings are oriented slightly closer to 90 degrees than the other two. The distorted cone shaped conformation is stabilized by two intramolecular O–H···O hydrogen bonds between proximal fragments on the lower rim, with O1···O2 distances of 2.65 Å (hydrogen bond length 1.85 Å), and O3···O4 distances of 2.77 Å (hydrogen bond length 1.95 Å).
28. O. Mitsunobu, M. Yamada and T. Mukaiyama, *Bull. Chem. Soc. Jpn.*, 1967, **40**, 935–939.
29. C. Ahn and P. DeShong, *J. Org. Chem.*, 2002, **67**, 1754–1759.
30. The X-ray structure contains four hydrogen bonds between neighboring OH–O and NH–O groups in the molecule. Low field ^{1}H NMR spectroscopic resonances of NH photons at 7.43 ppm are consistent with the presence these NH–O hydrogen bonds in solution also. The unit cell contains four molecules of ethanol, three of which are ordered, and the last being grossly disordered in the structure. The calixarene is observed to be in a flattened cone conformation, with dihedral angles of 70° and 68° for substituted aromatic rings with the main molecular plane that is formed by the four methylene bridges; and 53° and 45° for hydroxyl-containing aromatic rings relative to the same plane.
31. W. B. Jennings, *Chem. Rev.*, 1975, **75**, 307–322.
32. A. Arduini, M. Fabbi, M. Mantovani, L. Mirone, A. Pochini, A. Secchi and R. Ungaro, *J. Org. Chem.*, 1995, **60**, 1454–1457.
33. H. Takagi, T. Mizutani, T. Horiguchi, S. Kitagawa and H. Ogoshi, *Org. Biomol. Chem.*, 2005, **3**, 2091–2094; H.-J. Kim, S. Sakamato, K. Yamaguchi and J.-I. Hong, *Org. Lett.*, 2003, **5**, 1051–1054; H. Fenniri, B.-L. Deng and A. Ribbe, *J. Am. Chem. Soc.*, 2002, **124**, 11064–11072; S. R. Nam, H. J. Kim, S. Sakamato, K. Yamaguchi and J. I. Hong, *Tetrahedron Lett.*, 2004, **45**, 1339–1342.
34. C. Diedrich and S. Grimme, *J. Phys. Chem. A*, 2003, **107**, 2524–2539.
35. M. J. Frisch, G. W. Trucks, H. B. Schlegel, G. E. Scuseria, M. A. Robb, J. R. Cheeseman, J. A. Montgomery, Jr, T. Vreven, K. N. Kudin, J. C. Burant, J. M. Millam, S. S. Iyengar, J. Tomasi, V. Barone, B. Mennucci, M. Cossi, G. Scalmani, N. Rega, G. A. Petersson, H. Nakatsuji, M. Hada, M. Ehara, K. Toyota, R. Fukuda, J. Hasegawa, M. Ishida, T. Nakajima, Y. Honda, O. Kitao, H. Nakai, M. Klene, X. Li, J. E. Knox, H. P. Hratchian, J. B. Cross, V. Bakken, C. Adamo, J. Jaramillo, R. Gomperts, R. E. Stratmann, O. Yazyev, A. J. Austin, R. Cammi, C. Pomelli, J. W. Ochterski, P. Y. Ayala, K. Morokuma, G. A. Voth, P. Salvador, J. J. Dannenberg, V. G. Zakrzewski, S. Dapprich, A. D. Daniels, M. C. Strain, O. Farkas, D. K. Malick, A. D. Rabuck, K. Raghavachari, J. B. Foresman, J. V. Ortiz, Q. Cui, A. G. Baboul, S. Clifford, J. Cioslowski, B. B. Stefanov, G. Liu, A. Liashenko, P. Piskorz, I. Komaromi, R. L. Martin, D. J. Fox, T. Keith, M. A. Al-Laham, C. Y. Peng, A. Nanayakkara, M. Challacombe, P. M. W. Gill, B. Johnson, W. Chen, M. W. Wong, C. Gonzalez and J. A. Pople, *Gaussian 03*, Gaussian, Inc., Wallingford, CT, 2004.
36. J. R. Cheeseman, G. W. Trucks, T. A. Keith and M. J. Frisch, *J. Chem. Phys.*, 1996, **104**, 5497–5509.
37. Y. Cao, M. D. Beachy, D. A. Branden, L. Morrill, M. N. Ringnalda and R. A. Friesner, *J. Chem. Phys.*, 2005, **122**, 224116–224126.
38. SMART: Area-Detector Software Package, Bruker Analytical X-ray Systems, Inc., Madison, WI, 2001–03.
39. SIR97: A new tool for crystal structure determination and refinement, *J. Appl. Crystallogr.*, 1998.
40. DIRDIF-94: The DIRDIF-94 program system, Technical Report of the Crystallography Laboratory, University of Nijmegen, The Netherlands, 1994.
41. D. T. Cromer and J. T. Waber, *International Tables for X-ray Crystallography*, The Kynoch Press, Birmingham, England, 1974, vol. IV, Table 2.2A.
42. J. A. Ibers and W. C. Hamilton, *Acta Crystallogr.*, 1964, **17**, 781.
43. D. C. Creagh and W. J. McAuley, *International Tables for Crystallography*, ed. A. J. C. Wilson, Kluwer Academic Publishers, Boston, 1992, vol. C, Table 4.2.6.8, pp. 219–222.
44. D. C. Creagh and J. H. Hubbell, *International Tables for Crystallography*, ed. A. J. C. Wilson, Kluwer Academic Publishers, Boston, 1992, vol. C, Table 4.2.4.3, pp. 200–206.
45. *teXsan: Crystal Structure Analysis Package*, Molecular Structure Corporation, The Woodlands, Texas, 1992.